Doppler-free Stark spectroscopy of the second excited level of atomic hydrogen for measurements of electric fields

Minja Gemišić Adamov, Andreas Steiger,* Klaus Grützmacher, and Joachim Seidel
Physikalisch-Technische Bundesanstalt, Abbestraße 2-12, 10587 Berlin, Germany
(Received 31 July 2006; published 11 January 2007)

The Stark splitting of the second excited level of atomic hydrogen (with principal quantum number $n=3$) has been measured by pulsed laser spectroscopy in order to determine small electric fields by optical means. Doppler-free excitation with two counterpropagating laser beams at 205 nm allows us to measure the $n=3$ Stark spectra either by an optogalvanic signal after ionization by a third laser photon or by detection of the Balmer-α fluorescence photons emitted by the excited atoms. Three different cases of laser polarization have been investigated in order to evaluate the possibilities and limitations of this one-step laser excitation method for electric field determination, especially at field strengths below 200 V/cm. The method provides the best field sensitivity achieved with lower excited levels that can be reached directly by two-photon absorption from the ground state (in contrast to the more sensitive Rydberg levels). For this purpose, an advanced tunable pulsed uv laser with narrow bandwidth almost at the Fourier limit has been used. The high spectral resolution allowed us to deduce electric field strengths as small as 50 V/cm from the frequency shift between two selected isolated Stark components. As a main advantage, this simple analysis of the measured spectra does not rely on knowledge of the line intensities which may be strongly affected by the measuring conditions.

DOI: 10.1103/PhysRevA.75.013409 PACS number(s): 32.60.+i, 42.62.Fi, 42.65.Ky, 52.70.Kz

I. INTRODUCTION

One of the major requirements of gas discharge diagnostics is the determination of electric field strength distributions, which are often the key to understanding and controlling the plasma behavior. As the driving force accelerating the charged particles, the electric field is closely connected to other parameters such as charge density, energy distribution, flux of ions and electrons, and surface conditions. Therefore a knowledge of the field distribution is of particular interest for glow discharges, plasma switches, flames, and edge regions of high-temperature fusion plasmas, and also for optimizing the processing parameters of technological low-temperature plasmas.

Many techniques have been developed for electric field measurement, but nonintrusive optical spectroscopic methods provide the best sensitivity. In particular, pulsed laser spectroscopy allows for measurements with spatial and temporal resolutions of a few micrometers and nanoseconds, respectively. The electric field is optically determined from the changes in the structure of atomic or molecular spectra introduced by the Stark effect [1]. With laser photons, measured species are usually excited to a selected field-sensitive Rydberg state from the ground state or from a long-living metastable state. As their Stark effect is easy to calculate, helium atoms are often applied as field-sensitive "spectators," using, for example, the $n=11$ Rydberg state and optogalvanic detection [2,3]. Higher states are observed for better field sensitivity [4,5]. The spatial resolution is improved with laser-induced fluorescence detection [6–10]. Another method based on the change of polarization of fluorescent light in helium has been proposed for the edge region of a tokamak plasma [11,12]. Measurements are also performed with Ar atoms using calculated [13,14] or calibrated field dependence [15–17]. Heteronuclear diatomic molecules such as BCl [18,19], NaK [20–23], or BH [24] have also been used.

The hydrogen atom is probably the most prominent candidate as an optical probe for electric field detection: Its excited levels are highly sensitive to electric fields, the theory of its Stark splitting has been well known for a long time ([25] and references therein), and it is present anyway in many plasmas of industrial interest. Several different measurement techniques have been developed for atomic hydrogen. For instance, Doppler-free laser polarization spectroscopy [26] was demonstrated by observing the Stark splitting of the hydrogen Balmer-β line. The Stark structure of the Lyman-α transition [27] was studied with a pulsed laser system. With (2+1)-photon excitation [28] the Stark spectra of the $n=6$ level were measured by observation of indirectly induced Balmer-α fluorescence. An even more sensitive method [29–31] first uses Doppler-free two-photon excitation to the $n=3$ level, and then observes the decrease of the Balmer-α fluorescence by depopulating this level with an additional infrared laser tuned across high-lying Rydberg states. Two other methods have recently been presented, the first one using two-photon polarization spectroscopy of the Stark-split $n=2$ level of deuterium [32] and the second one observing two-step-resonant excited Stark spectra of the $n=8$ level of hydrogen [24].

The measurement scheme used here, with two 205 nm laser photons exciting hydrogen from its ground level to the $n=3$ level and observation of the induced Balmer-α emission (Fig. 1), gives the largest number of fluorescence photons per incident laser photon in comparison with other schemes [33]. This scheme was previously applied for various measurements mostly determining atomic number densities in different plasma sources and flames [34–43]. In Ref. [44] the scheme was also applied for electric field measurements. The authors used laser beams linearly polarized parallel to the

*Electronic address: Andreas.Steiger@PTB.de

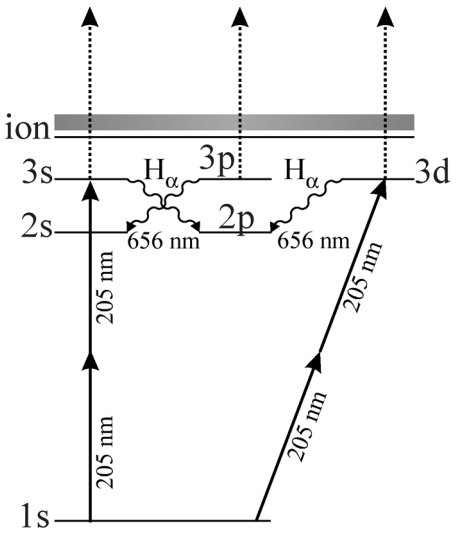

FIG. 1. Energy levels of atomic hydrogen and the transition schemes important for the measuring method.

external electric field for their measurements, but expected better sensitivity with laser beams polarized perpendicular to the field.

In this paper, we present a detailed investigation of this approach which provides an easily applicable method for detecting local electric field strengths. In particular, we determined a single field-sensitive parameter of the two-photon absorption spectrum and studied its dependence on the laser polarization by experiment. In addition to linear polarizations parallel and perpendicular to the electric field, we also employed circular polarization of both beams, which yields a two-photon Stark spectrum independent of the field direction. For the detection of two-photon absorption, two concurrent subsequent processes depopulating the excited $n=3$ level were used (Fig. 1): ionization by a third laser photon and radiative decay to the $n=2$ level, i.e., Balmer-α fluorescence [34,39,43,45]. The current pulse of charged particles produced by the laser pulse is measured by an optogalvanic (OG) detection scheme simultaneously with the laser-induced fluorescence (LIF) signal. Another minor concurrent process is stimulated emission [39,45] sporadically seen by eye in this experiment.

The narrowband pulsed radiation at 205 nm for two-photon excitation was produced by a special solid-state laser system developed in our laboratory [46]. The idea was to use advantages of this precisely tunable system with nanosecond pulse duration and nearly Fourier-limited bandwidth in this experiment in order to yield directly the Stark-split spectra. At the cost of a small loss in sensitivity, the simple measuring scheme avoids any extra excitation with an additional laser and the complexity of the Rydberg spectra [29] as well.

II. THEORETICAL BACKGROUND OF THE MEASURING METHOD

In general, the higher excited atomic levels are more sensitive to external electric fields than the lower levels. For the hydrogen atom, the Stark splitting scales approximately with the square of the principal quantum number n. Therefore the observation of highly excited (Rydberg) levels seems to be most suitable for the determination of electric field strengths. However, the excitation of these levels from the hydrogen ground state is experimentally rather demanding: Even two-photon laser excitation gives direct access only to $n=2$ and 3. Higher levels would require laser wavelengths below 200 nm in the vacuum ultraviolet spectral range, where tunable laser radiation cannot be generated with good performance. Because of this, the higher levels are usually excited via $n=2$ or 3 with an additional second laser [28,29]. This increases the complexity of the experimental setup significantly. In addition, the Stark spectra of highly excited levels consist of many components, and since single components are seldom resolved, whole spectra have to be compared with theoretical results in order to obtain electric field values.

These disadvantages are avoided if the electric field is determined from the Stark splitting of the $n=2$ or 3 level. Of these, the $n=3$ level is more difficult to excite, but provides the better field sensitivity and the favorable possibility of laser-induced-fluorescence detection in the visible spectral range (Fig. 1). Doppler-free spectra exhibit clearly resolved Stark components and offer the opportunity of choosing an individual pair of components the frequency splitting of which is field sensitive. Such a frequency difference can be measured precisely and allows for electric field determination by direct comparison with theory.

The properties of the Stark spectra of the $n=3$ level relevant for the desired application are briefly summarized here. The corresponding calculations took into account the hyperfine splitting of the ground level, but neglected the small hyperfine splitting of the excited $n=3$ level. With this simplification, all spectral line components have the same doublet structure: a weak hyperfine component on the high-frequency side of each strong component with a 1:3 intensity ratio, the frequency shift being the hyperfine splitting of the ground level, namely, 710 MHz at the laser wavelength of 205 nm. This is consistent with the measured spectra (see Sec. IV). Because the splitting is the same for all Stark components, the hyperfine components are not shown separately in Fig. 2 for the sake of greater clarity.

The Stark splitting is illustrated in Fig. 2 for the electric field interval of interest. In addition to the Stark-split energy eigenvalues [Fig. 2(a)], the effect of the mixing of the $n=3$ states on the two-photon absorption rate (or "relative probability" of two-photon absorption) from the ground state is also shown. This probability depends on the polarization of the laser beams used for excitation. Results are shown for the three cases of laser polarization investigated in this work: linear polarization either perpendicular (s polarization) or parallel (p polarization) to the electric field, and circular polarization exciting the $\Delta m=0$ transitions. The results are shown in Figs. 2(b), 2(c), and 2(d), respectively. For zero electric field, only transitions to $3S$ and $3D$ states are allowed by the two-photon-absorption selection rule $\Delta l=0$ or 2. Due to the mixing of unperturbed states with increasing electric field, the Stark component corresponding to the transition to the states evolving from the original $3P_{1/2}$ states (denoted as the "$3P_{1/2}$ component" for brevity, and similarly for other components) appears and increases at the expense of the

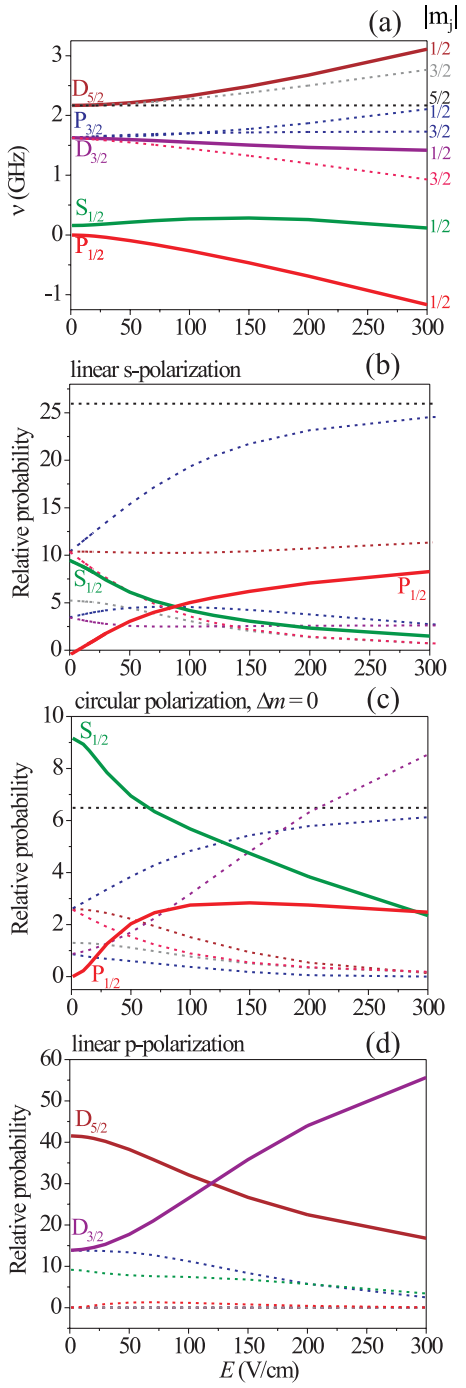

FIG. 2. (Color online) Calculated Stark splitting of the $n=3$ level of hydrogen as a function of the electric field. (a) Energy levels are presented as offset of the laser frequency from the unperturbed $3P_{1/2}$ component. Individual Stark components are labeled by the absolute value $|m_j|$ of the projection of the total angular momentum to the field direction. (b), (c), and (d) Relative probability of all Stark components for the different cases of laser polarizations. The components selected for field determination are emphasized with solid lines.

$3S_{1/2}$ component. Because of the fine-structure splitting these two components are clearly separated from the other ones, and their frequency separation, increasing from the Lamb shift at zero electric field, is suitable for electric field determination. This applies to circular and s polarization, Figs. 2(b) and 2(c). The Stark components of the other $n=3$ fine-structure levels originating from $3D_{5/2}$, $3D_{3/2}$, and the (zero-field-forbidden) $3P_{3/2}$ are close together in frequency, Fig. 2(a). Since almost all components of this manifold have significant intensities in the electric field range of interest, Figs. 2(b) and 2(c), they cannot be easily separated.

In the case of linear p polarization, Fig. 2(d), the situation is completely different. The originally forbidden $3P_{1/2}$ component remains very weak in the whole electric field range of interest. On the other hand, only two of all the $3D_{5/2}$, $3D_{3/2}$, and $3P_{3/2}$ components are significant, namely, $3D_{5/2,1/2}$ and $3D_{3/2,1/2}$. The first one decreases and the second one increases with increasing electric field. Their frequency separation, Fig. 2(a), increases with the field strength from the fine-structure value at zero electric field and can be used as a field measure.

The Stark components selected for the measurement of electric field strengths are emphasized with solid lines in Fig. 2. Their calculated frequency splitting values are used for comparison with the experimental results.

III. EXPERIMENT

A. Laser system

The main principles of tunable pulsed solid-state lasers based on a special concept of efficient frequency conversion into the ultraviolet spectral range are described in Ref. [47]. The laser system generating 205 nm radiation (Fig. 3) was developed in our laboratory. Some improvements of the first setup [46,48] had to be implemented to obtain the high performance necessary for precise, high-resolution two-photon spectroscopy. As the laser is the key element for our measuring method, it is briefly described.

Tunable pulsed radiation is generated by frequency splitting of the second harmonic of a Q-switched, injection-seeded neodymium-doped yttrium aluminum garnet (Nd:YAG) laser in a pulsed optical parametric oscillator (OPO). The wavelengths of signal and idler photons are defined by the phase-matching condition of the parametric process. Because of its favorable nonlinear properties, angle-tuned potassium titanyl phosphate (KTP) was chosen as the OPO crystal. The short OPO resonator for the signal radiation consists of the KTP crystal placed between two plane mirrors highly reflective for the signal radiation. Single-longitudinal-mode pulsed operation is achieved by injection seeding with an external-cavity cw diode laser operated at the signal wavelength. The special feature of the OPO is its frequency tuning performed by changing the cavity length in a controlled way. One resonator mirror is mounted on a translation stage with frictionless flexure guidance at a controlled distance variable with nanometer precision by capacitive sensors. In contrast to other approaches the diode laser is frequency locked to the cavity length. In that way, good linearity of the frequency tuning is provided by changing the position of the mirror. The OPO generates nearly 1 mJ pulse energy in 5.5 ns at 820 nm, continuously tunable over a range of 50 GHz.

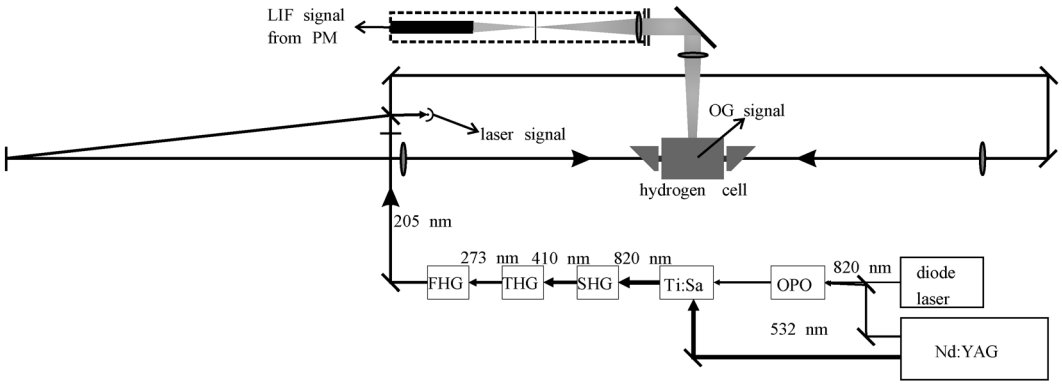

FIG. 3. Scheme of the laser system at 205 nm and the experimental setup. Simultaneous detection of the LIF and OG signals and the laser pulse energy is denoted. PM denotes the photomultiplier, Ti:Sa a Ti:sapphire laser, and SHG, THG, and FHG second-, third-, and fourth-harmonic generation.

The OPO pulse is amplified in two Ti:sapphire crystals pumped by the major part of the second harmonic of the Nd:YAG laser. In the improved setup, six-pass amplification in the first crystal is followed by two-pass amplification in the second crystal.

The amplified 820 nm radiation with up to 60 mJ pulse energy is converted into its fourth harmonic by stepwise sum-frequency generation via the second, third, and fourth harmonics using three Beta-barium borate (BBO) crystals. This is about ten times more efficient than frequency doubling of the second harmonic, because phase matching of the latter process would require a BBO crystal with an unfavorable cutting angle of nearly 90°. With the stepwise sum-frequency generation, 5 mJ pulse energy in less than 4 ns with a spectral bandwidth of about 300 MHz are achieved at 205 nm. In addition to the high pulse energy and the narrow bandwidth, the modified system provides good pulse-to-pulse reproducibility and scan linearity, which are important for precise Doppler-free two-photon laser spectroscopy.

A moderate pulse energy of 1.5 mJ is used in the experiment. The 205 nm laser beam is divided by a beam splitter, and the two beams are directed to counterpropagate into the measuring cell. Both beams are focused with 1 m lenses, and the measurement volume is 20 cm before the foci of the beams. In the center of the measurement volume, the beam diameters are about 1 mm, resulting in a laser irradiance of about 50 MW/cm^2, which is sufficient for the Doppler-free excitation of hydrogen atoms, but does not cause significant power broadening or dominant photoionization.

B. Hydrogen cell

The measurements were performed in a small vacuum cell filled with hydrogen gas at a pressure of about 300 Pa. The design of the cell is shown in Fig. 4. Hydrogen molecules are thermally dissociated by a tungsten filament 1.5 mm in diameter, heated by a dc current of about 90 A. The hot wire is connected to a dc voltage defining the electric field together with another grounded wire mounted in parallel at a distance of about 8 mm. In the case of optogalvanic detection, the grounded wire also serves as pickup electrode for the hydrogen ions produced by the laser pulse directly after resonant two-photon excitation of the atoms. The exactly counterpropagating laser beams are aligned parallel to both wires in their midplane, where the electric field strength is constant due to the symmetry of the arrangement.

The quartz windows of both end caps of the cell are mounted at the Brewster angle for linearly polarized laser beams (Fig. 4). In the case of circular polarization, the end caps are replaced by quartz windows nearly normal to the beams. On the side of the cell, a window allows to observe the laser-induced fluorescence signal perpendicular to the laser beams. In order to reduce the stray light from the hot filament, a slit aperture is mounted inside the cell at the height of the laser beams.

C. Measurement procedure

Absorption of two counterpropagating 205 nm photons results in Doppler-free excitation of ground-state hydrogen atoms to the $n=3$ level. Some of the excited atoms emit Balmer-α radiation at 656.3 nm ($n=3$ to $n=2$ transition) with a high branching ratio. A lens collects this laser-induced

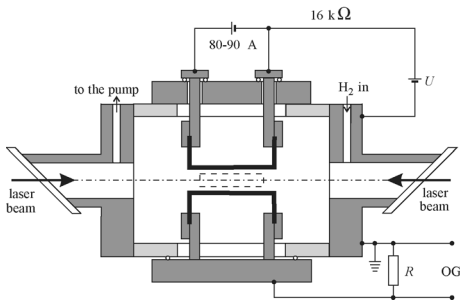

FIG. 4. Schematic sectional drawing of the low-pressure hydrogen cell made of an aluminum housing (light gray) covered with water-cooled brass flanges (dark gray). The electric field between the hot filament (top) and the pickup wire (bottom) is established by applying a variable dc voltage U of up to 300 V through a 16 kΩ load resistor. The fluorescence signal is observed through a window on the back side of the cell (dashed rectangle). The optogalvanic signal is produced by the ion current to the pickup wire as it flows to the ground level through the resistor R.

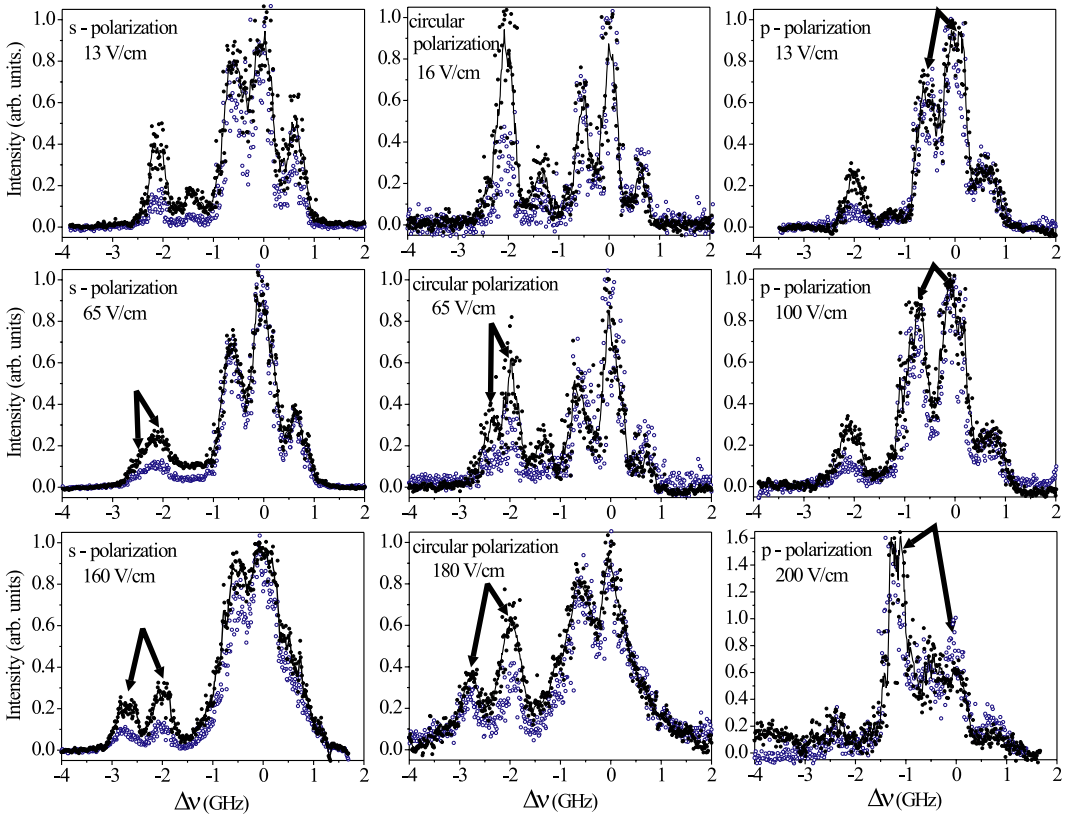

FIG. 5. (Color online) Measured spectra of the two-photon excited $n=3$ level of hydrogen for different electric field strengths and three different laser polarizations. Dots indicate the OG signal and open circles the LIF signal. The frequency scale is in GHz at the 205 nm wavelength of the laser. The two selected components for field determination are indicated by arrows.

fluorescence radiation into a parallel beam, which passes through two subsequent interference filters ($\lambda=656$ nm, $\Delta\lambda=10$ and 5 nm) and is refocused by a second lens to a spatial slit filter improving the spatial resolution of electric field measurements (Fig. 3). The narrow slit width is aligned to image the center of the laser beams, and the slit length limits the optical detection volume to a region of homogeneous field strength inside the cell. Behind the filter, the diverging light illuminates the photocathode of a photomultiplier optimized for linearity in pulsed operation.

Another part of the excited hydrogen atoms is ionized by absorption of a third laser photon, a nonlinear process enhanced by the two-photon resonance. The charged particles resulting from this are separated by the electric field. The ions are collected by the pickup wire. The resulting charge pulse is amplified and measured as optogalvanic signal.

Both signals (from the photomultiplier and the OG amplifier) and the laser pulse energy at 205 nm (measured by a photodiode) are sampled and recorded by a computer at the 10 Hz repetition rate of the laser. Each data point represents the recordings of a single laser pulse while tuning the laser frequency. The final spectrum is obtained as the mean value of a forward and a backward scan of the laser.

OG and LIF measurements were performed simultaneously for the three different cases of laser polarization applied. The laser polarization was varied by introducing half-wave or quarter-wave plates in the counterpropagating laser beams.

IV. RESULTS AND DISCUSSION

Results of the measurements are shown in Figs. 5 and 6. In Fig. 5, examples of the measured spectra are presented for the three cases of laser polarization and three different electric field values. Both of the spectra obtained by fluorescence (LIF) and optogalvanic detection are shown. The OG signal detection requires a certain minimum electric field for charged particles to be collected by the pickup wire. LIF measurements are possible also for zero fields.

In the case of very weak fields, the spectra consist of $3S$ and $3D$ components only. The weak component on the low-frequency side corresponds to the $3S_{1/2}$ and the stronger components correspond to the $3D_{3/2}$ and $3D_{5/2}$ fine-structure sublevels of the $n=3$ level. The hyperfine structure, largely due to the hyperfine splitting of the $1S$ ground level, introduces an additional weak component on the high-frequency side of each component. Only five components show up in the spectra because the weak hyperfine component of $3D_{3/2}$ is hidden under the strong $3D_{5/2}$ component. With zero electric field, the spectra should be identical for p and s polarization. The small difference of OG spectra in very weak electric fields is attributed to slightly different measuring conditions and the fact that ions produced in such weak fields are only partly collected. The $3S_{1/2}$ component is much stronger for $\Delta m=0$ circular polarization, as expected. In the OG spectrum, the $3S_{1/2}$ component is always stronger than in the LIF spectrum (with the $3D$ components normalized to the

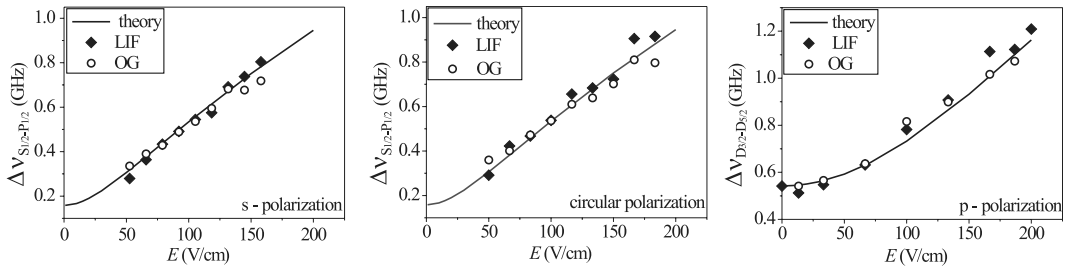

FIG. 6. Measured and calculated frequency separation between the two selected components suitable for electric field measurements at different electric field strengths and the three cases of laser polarization.

same intensity). This is due to the different transition probabilities for the LIF and OG processes taking place after two-photon absorption. For the LIF signal (Balmer-α emission), the radiative transition probability from $3S$ to $2P$ is ten times smaller than the transition probability from $3D$ to $2P$ [34]. In contrast, ionization by a third laser photon leading to the OG signal has practically the same probability for all sublevels.

Comparing OG and LIF detection, we point out that OG detection has higher sensitivity (signal-to-noise ratio). On the other hand, LIF detection perpendicular to the laser beams provides better spatial resolution: While the OG signal is averaged along the whole overlap region of the two laser beams or the region from where charged particles can reach the pickup wire, LIF is detected only from the restricted area defined by the spatial filter in the fluorescence detection channel. The line widths were not found to be significantly broader in the OG spectra than in the LIF spectra, in accordance with a similar comparison [9].

The measured spectra were found to be consistent with the theoretical predictions. For circular and s polarization, the originally forbidden $3P_{1/2}$ component appears on the low-frequency side of the $3S_{1/2}$ component, its shift and intensity increasing with the electric field. These two components stay separated from the $3D_{3/2}$, $3D_{5/2}$, and $3P_{3/2}$ components which are unresolved in the fields of interest. The frequency shift between the $3P_{1/2}$ and $3S_{1/2}$ line components is compared with calculated results for the electric field determination (Fig. 6). The lower field detection limit of about 50 V/cm is reached when the $3P_{1/2}$ component is just distinguishable from the $3S_{1/2}$ component; hence the laser bandwidth plays a key role.

As predicted in the case of p polarization, the $3P_{1/2}$ component does not appear in the spectrum. Also the $3D_{3/2}$, $3D_{5/2}$, and $3P_{3/2}$ manifold is reduced to only two clearly resolved Stark components with their well-known hyperfine structure. For p polarization and electric fields of about 200 V/cm, we can even resolve the weak hyperfine component between the two observed strong components (Fig. 5). The frequency shift between the $3D_{3/2}$ and $3D_{5/2}$ components is a suitable measure for the electric field strength. Although both components remain allowed at zero field, the weak dependence of the frequency shift on small electric fields (Fig. 6) sets a practical field detection limit similar to the 50 V/cm limit for the other cases of polarization.

To obtain the exact frequency position of the interesting components in the measured spectra, all components were fitted with Gaussian profiles of the same spectral width. The weak hyperfine components are always included in the fit procedure with a fixed frequency separation of 710 MHz and an intensity ratio of 1:3, even if they are unresolved. The Stark shift values are evaluated from the positions of the strong components.

The dependence of the frequency shift on the electric field strength is shown in Fig. 6 for the three measured polarization conditions. The solid lines represent the calculated values, the dots are the results extracted from the measured spectra. The solid diamonds represent the LIF data and the empty circles the OG data. There is no significant difference between the results of the two detection methods. Discrepancies of the OG and LIF data and deviations from the theoretical curve are attributed to residual field inhomogeneities and imperfections of the laser frequency tuning. The data evaluation contributes additional noise by the fit procedure used to determine the frequency position of the Stark components in the measured spectrum. The total estimated relative uncertainty varies from 8% for medium field values to 20% for weak fields when components are hardly resolved and 15% for high fields when components are broadened due to the field inhomogeneity.

V. CONCLUSION

In this paper the practicability of a simple, sensitive optical method for local electric field measurements in plasmas containing hydrogen atoms has been investigated in detail. The method requires only a single laser for Doppler-free two-photon excitation of ground-state atoms and direct observation of the Stark splitting of the excited level.

The Stark splitting of $n=3$ level of hydrogen is well suited for this purpose, but a laser system with high performance providing pulsed radiation with narrow bandwidth tunable around 205 nm is essential for its successful application. Such a system was developed in our laboratory, and the measurements described here prove its applicability for high-resolution nonlinear laser spectroscopy.

The spectral dependence of the resonant two-photon absorption was measured simultaneously by two different techniques: Balmer-α fluorescence and an optogalvanic signal. Both fluorescence and optogalvanic spectra give good results in comparison with theoretical values for the Stark splitting of the $n=3$ level. Therefore, the detection method can in principle be chosen according to the requirements of the gas discharge to be examined. In general, fluorescence detection

is considered to be more advantageous, because optogalvanic detection has only limited spatial resolution and may disturb the discharge.

Analysis of the measured spectra revealed the frequency separation of two Stark components as the parameter most suitable for electric field determination in the three cases of laser polarization investigated. As compared to other methods which require comparison of the whole measured spectrum with a set of theoretically calculated spectra, our approach is more simple and straightforward without significant loss of sensitivity. The main advantage of determining the electric field strength from the frequency difference is that this does not rely on critical line intensity information such as varying fluorescence yields or collisional quenching of different Stark components.

A lower field detection limit of about 50 V/cm was verified for each of the three measured cases of laser polarization. Compared to linear *p* or *s* polarization, circularly polarized beams exciting the $\Delta m=0$ two-photon transitions lead to a sensitivity independent of the field direction.

Based on the results of this investigation, we recommend the one-step laser excitation method presented here for further use in plasma diagnostics for sources containing hydrogen. The high pulse energy of the laser even opens the possibility for sheet diagnostics with nanosecond time resolution and a spatial resolution defined by an appropriate fluorescence detection system. The narrow bandwidth of the laser allows the electric field to be determined with an uncertainty of about 10 V/cm.

[1] J. E. Lawler and D. A. Doughty, Adv. At., Mol., Opt. Phys. **34**, 171 (1994).
[2] D. K. Doughty and J. E. Lawler, Appl. Phys. Lett. **45**, 611 (1984).
[3] E. A. Den Hartog, D. A. Doughty, and J. E. Lawler, Phys. Rev. A **38**, 2471 (1988).
[4] B. N. Ganguly and A. Garscadden, Appl. Phys. Lett. **46**, 540 (1985).
[5] B. N. Ganguly, J. Appl. Phys. **60**, 571 (1986).
[6] K. E. Greenberg and G. A. Hebner, Appl. Phys. Lett. **63**, 3282 (1993).
[7] G. A. Hebner, K. E. Greenberg, and M. E. Riley, J. Appl. Phys. **76**, 4036 (1994).
[8] M. D. Bowden, Y. W. Choi, K. Muraoka, and M. Maeda, Appl. Phys. Lett. **66**, 1059 (1995).
[9] B. N. Ganguly and D. A. Dolson, Plasma Sources Sci. Technol. **9**, 437 (2000).
[10] J. B. Kim, T. Ikutake, M. D. Bowden, K. Muraoka, and U. Czarnetzki, Jpn. J. Appl. Phys., Part 1 **39**, 299 (2000).
[11] T. Oda and K. Takiyama, in Proceedings of the Seventh International Symposium on Laser-Aided Plasma Diagnostics (Fukuoka, Japan, 1995), edited by K. Muraoka (unpublished), p. 227.
[12] K. Takiyama, T. Katsuta, M. Watanabe, S. Li, T. Oda, T. Ogawa, and K. Mizuno, Rev. Sci. Instrum. **68**, 1028 (1997).
[13] V. P. Gavrilenko, H. J. Kim, T. Ikutake, J. B. Kim, Y. W. Choi, M. D. Bowden, and K. Muraoka, Phys. Rev. E **62**, 7201 (2000).
[14] V. P. Gavrilenko, H. J. Kim, T. Ikutake, J. B. Kim, M. D. Bowden, and K. Muraoka, Phys. Rev. E **63**, 047401 (2001).
[15] Y. W. Choi, M. D. Bowden, and K. Muraoka, Appl. Phys. Lett. **69**, 1361 (1996).
[16] E. V. Barnat and G. A. Hebner, in Proceedings of the 12th International Symposium on Laser-Aided Plasma Diagnostics (Snowbird, UT, 2005), edited by N. Luhmann (unpublished), p. 41.
[17] K. Takizawa, K. Sasaki, and K. Kadota, Jpn. J. Appl. Phys., Part 1 **41**, L1285 (2002).
[18] C. A. Moore, G. P. Davis, and R. A. Gottscho, Phys. Rev. Lett. **52**, 538 (1984).
[19] Y. Yamagata, Y. Kawano, K. Muraoka, M. Maeda, and M. Akazaki, Jpn. J. Appl. Phys., Part 1 **30**, 166 (1991).
[20] J. Derouard and N. Sadeghi, Opt. Commun. **57**, 239 (1986).
[21] H. Debontride, J. Derouard, P. Edel, R. Romestain, N. Sadeghi, and J. P. Boeuf, Phys. Rev. A **40**, 5208 (1989).
[22] M. P. Alberta, H. Debontride, H. Derouard, and N. Sadegi, J. Phys. III **3**, 105 (1993).
[23] Y. Takahashi, T. Yoshino, and K. Kawasaki, Jpn. J. Appl. Phys., Part 1 **35**, 2334 (1996).
[24] E. V. Cherkasova, V. P. Gavrilenko, and A. I. Zhuzhunashvili, J. Phys. D **39**, 477 (2006).
[25] G. Lüders, Ann. Phys. (Leipzig) **8**, 301 (1951).
[26] C. Wieman and T. W. Hänsch, Phys. Rev. Lett. **36**, 1170 (1976).
[27] L. Cabaret, C. Delsart, and C. Blondel, Opt. Commun. **61**, 116 (1987).
[28] J. P. Booth, M. Fadlallah, J. Derouard, and N. Sadeghi, Appl. Phys. Lett. **65**, 819 (1994).
[29] U. Czarnetzki, D. Luggenhölscher, and H. F. Döbele, Phys. Rev. Lett. **81**, 4592 (1998).
[30] U. Czarnetzki, D. Luggenhölscher, and H. F. Döbele, Plasma Sources Sci. Technol. **8**, 230 (1999).
[31] U. Czarnetzki, D. Luggenhölscher, and H. F. Döbele, Appl. Phys. A: Mater. Sci. Process. **72**, 509 (2001).
[32] M. I. de la Rosa, C. Perez, K. Grützmacher, A. B. Gonzalo, and A. Steiger, Plasma Sources Sci. Technol. **15**, 105 (2006).
[33] U. Czarnetzki, K. Miyazaki, T. Kaiwara, K. Muraoka, M. Maeda, and H. F. Döbele, J. Opt. Soc. Am. B **11**, 2155 (1994).
[34] H. W. P. van der Heijden, M. G. H. Boogaarts, S. Mazouffre, J. A. M. van der Mullen, and D. Schram, Phys. Rev. E **61**, 4402 (2000).
[35] J. E. M. Goldsmith and L. A. Rahn, Opt. Lett. **15**, 814 (1990).
[36] P. Verkerk, M. Pinard, F. Biraben, and G. Grynberg, Opt. Commun. **72**, 202 (1989).
[37] R. P. Lucht, J. T. Salamon, G. King, D. Sweeney, and N. Laurendeau, Opt. Lett. **8**, 365 (1983).
[38] J. Bokor, R. R. Freeman, J. C. White, and R. H. Storz, Phys. Rev. A **24**, 612 (1981).
[39] J. Amorim, G. Baravian, M. Touzeau, and J. Jolly, J. Appl. Phys. **76**, 1487 (1994).
[40] J. E. M. Goldsmith, Opt. Lett. **11**, 416 (1986).
[41] U. Meier, K. Kohse-Höinghaus, L. Schäfer, and C. P. Klages,

Appl. Opt. **29**, 4993 (1990).
[42] H. Umemoto, K. Ohara, D. Morita, Y. Nozaki, A. Masuda, and H. Matsumura, J. Appl. Phys. **91**, 1650 (2002).
[43] M. G. H. Boogaarts, S. Mazouffre, G. J. Brinkman, H. W. P. van der Heijden, P. Vankan, J. A. M. van der Mullen, D. Schram, and H. F. Döbele, Rev. Sci. Instrum. **73**, 73 (2002).
[44] J. P. Booth, J. Derouard, M. Fadlallah, L. Cabaret, and J. Pinard, Opt. Commun. **132**, 363 (1996).
[45] J. E. M. Goldsmith, J. Opt. Soc. Am. B **6**, 1979 (1989).
[46] A. Bustillo, Ph.D. thesis, Universidad de Valladolid, 2000 (unpublished).
[47] A. Steiger, K. Grützmacher, and M. I. de la Rosa, in *Laser in Research and Engineering*, edited by W. Waidelich (Springer-Verlag, Berlin, 1996), p. 308.
[48] A. Bustillo, K. Grützmacher, A. Steiger, and L. Werner, in Proceedings of the Tenth International Symposium on Laser-Aided Plasma Diagnostics (Fukuoka, Japan, 2001), edited by K. Muraoka (unpublished) p. 247.